Geoscientific
Model Development
Discussions

Open Access

RRAWFLOW: Rainfall-Response Aquifer and Watershed Flow Model (v1.11)

A. J. Long

US Geological Survey, 1608 Mountain View Rd, Rapid City, South Dakota, USA

Correspondence to: A. J. Long (ajlong@usgs.gov)

Abstract

The Rainfall-Response Aquifer and Watershed Flow Model (RRAWFLOW) is a lumped-parameter model that simulates streamflow, springflow, groundwater level, solute transport, or cave drip for a measurement point in response to a system input of precipitation, recharge, or solute injection. The RRAWFLOW open-source code is written in the R language and is included in the Supplement to this article along with an example model of springflow. RRAWFLOW includes a time-series process to estimate recharge from precipitation and simulates the response to recharge by convolution; i.e., the unit hydrograph approach. Gamma functions are used for estimation of parametric impulse-response functions (IRFs); a combination of two gamma functions results in a double-peaked IRF. A spline fit to a set of control points is introduced as a new method for estimation of nonparametric IRFs. Other options include the use of user-defined IRFs and different methods to simulate time-variant systems. For many applications, lumped models simulate the system response with equal accuracy to that of distributed models, but moreover, the ease of model construction and calibration of lumped models makes them a good choice for many applications. RRAWFLOW provides professional hydrologists and students with an accessible and versatile tool for lumped-parameter modeling.

1 Introduction

Hydrological models, commonly referred to as a "lumped-parameter" or "lumped" models, generally have a small number of parameters, each representing a property of the entire hydrological system; conceptually, many physical processes are lumped into a few parameters. The Rainfall-Response Aquifer and Watershed Flow Model (RRAWFLOW) is one such model that is partially based on unit-hydrograph theory (Nash, 1959). RRAWFLOW simulates a time-series record for a measurement point of streamflow, springflow, groundwater level, solute transport, or cave drip in response

to a system input of precipitation, recharge, or solute injection. A preliminary version of RRAWFLOW was developed by Long and Mahler (2013) and used to classify karst aquifers and characterize time-variant systems. This preliminary version also was used by Symtad et al. (2014) to simulate future scenarios of streamflow and groundwater
5 level in a cave in Wind Cave National Park, United States and by the U.S. Geological Survey to simulate future scenarios of springflow and groundwater level in two karst aquifers (http://txpub.usgs.gov/crsp1/).

   I present a new version of RRAWFLOW with additional options that include (1) the gamma function for parametric impulse-response functions (IRFs), (2) a spline curve
10 or straight-line segments fit through a set of control points for nonparametric IRFs, (3) any user-defined IRF, and (4) a new option for time-variant systems that uses a continuously changing IRF scale. To my knowledge, the spline-curve method previously has not been used for the IRF. Additional options for time-variant systems also are available in RRAWFLOW. The open-source code is written in the R language (http:
15 //www.r-project.org/index.html) and is included in the Supplement to this article.

   In contrast to lumped models, distributed models discretize the system into small compartments or cells, each of which has several parameters defined. All hydrological models, however, are lumped to some degree. Models that frequently are considered physically based simulate numerous small-scale physics by lumping these pro-
20 cesses into simplified mathematical forms (Beven, 1989). The use of the term "physically based" to describe any hydrological model, therefore, should be discouraged (Beven and Young, 2013). Both distributed and lumped models, however, have components that can represent different hydrological processes that can be interpreted in physically meaningful ways (Beven and Young, 2013). For example, the IRF estimated
25 in many lumped models represents the physical response to an impulse into the system and provides mechanistic insights into that system, including the peak response time and magnitude and the hydrological memory of the system (von Asmuth and Knotters, 2004; Beven and Young, 2013; Young, 2013). The IRF could be measured directly at the outflow point (e.g., a spring) if a short, intense recharge event follows a long, dry

RRAWFLOW

A. J. Long

period. Most commonly, however, the outflow, or system response, results from a series of superposed responses to repeating recharge events, and the lumped model is used to estimate the IRF iteratively and to simulate the system response.

In a comparison of lumped models to distributed models, Reed et al. (2004) concluded that lumped models had better overall performance than distributed models but also cited several other studies indicating that distributed or semi-distributed models may or may not provide improvement over lumped models. In another comparison similar to that of Reed et al. (2004), Smith et al. (2013) concluded that distributed models provided improvements over lumped models in 12–24 % of the cases tested, depending on the criteria of evaluation. The mixed results of these comparisons indicate that lumped models are a good choice when the objectives do not require a distributed model.

A major advantage of a lumped model is its ease of construction and calibration because of the small number of parameters to estimate and because there is no need to assemble large datasets representing the physical properties of the system. Lumped models are particularly applicable to karst aquifers, where the geometry of the conduit network frequently is unknown. Lumped models provide an efficient means to simulate the response to possible future changes in the system input (e.g., precipitation). The primary advantage of distributed models is to simulate the response to possible changes within the system, such as urban development or increased groundwater pumping, for example. The choice to use a lumped or distributed model, therefore, depends on a study's objectives and available resources; a lumped model likely is the better choice if it meets the study's objectives.

Time-variant and time-invariant systems were described by Jenkins and Watts (1968). For example, Larocque et al. (1998) described high-flow periods exhibiting distinctly different response characteristics from low-flow periods. RRAWFLOW has options to simulate time-variant systems that generally are not available in distributed watershed models (e.g., PRMS; http://wwwbrr.cr.usgs.gov/projects/SW_MoWS/PRMS.html). If a distributed model is required for a specific study, RRAWFLOW

might be useful as an exploratory tool to analyze the system's sensitivity to time-variant response characteristics. RRAWFLOW also could be a useful educational tool for hands-on instruction of some of the basic principles in hydrology. Herein, one springflow site and one groundwater-level site are used in several example applica-
5 tions that demonstrate model options and calibration and validation procedures. Input, output, and calibration files are available in the Supplement for one of these examples.

2   The model

Effective precipitation for a watershed is the amount of precipitation that results in streamflow exiting the watershed. This consists of infiltration to groundwater below the
10 root zone that reemerges as streamflow, shallow groundwater interflow, and overland runoff. Processes that apply to effective precipitation for watershed models also apply to infiltration recharge to groundwater that causes a response in springflow or ground-water level, except that overland runoff is not included in this case. In RRAWFLOW, the term "recharge" is used for both watershed modeling and groundwater modeling.
15 A daily time step is suitable for most applications. Time steps shorter than one day can be used for high-resolution simulations, but time steps longer than one day should not be used when estimating recharge with Eqs. (1)–(4). The response in springflow or groundwater level to recharge is simulated by the convolution integral (Jenkins and Watts, 1968; Smith, 2003). RRAWFLOW is independent of specific units for flow, wa-
20 ter level, or solute concentration, and the user should maintain unit consistency. Air temperature is always in °C.

2.1   Precipitation recharge

To estimate recharge from direct precipitation, a daily soil-moisture index s [unitless] is estimated. Quantitatively, s is the daily fraction of precipitation that infiltrates and
25 becomes recharge. To account for the antecedent effects of rainfall on soil moisture, the

RRAWFLOW

A. J. Long

Title Page

Abstract   Introduction

Conclusions   References

Tables   Figures

◀◀   ▶▶

◀   ▶

Back   Close

Full Screen / Esc

Printer-friendly Version

Interactive Discussion

past daily-rainfall record is weighted by a backward-in-time exponential decay function (Jakeman and Hornberger, 1993):

$$s_i = cr_i + \left(1 - \kappa_i^{-1}\right) s_{i-1} \tag{1}$$

$$= c \left[r_i + \left(1 - \kappa_i^{-1}\right) r_{i-1} + \left(1 - \kappa_i^{-1}\right)^2 r_{i-2} + \ldots \right]$$

$$i = 0, 1, \ldots, N \qquad 0 \geq s \geq 1,$$

where c [L^{-1}] is a coefficient that limits s to the range 0–1; κ [unitless] adjusts the effect of antecedent rainfall and is related to evapotranspiration; r is total daily rainfall [L]; and i is the time step, typically in days. In RRAWFLOW, this method is option 1 for system input (Table 1). For watershed modeling, the value of c can be set to satisfy the assumption that the total recharge volume within a watershed is equal to the total outflow volume for the calibration and validation periods. This assumption neglects the net change in total watershed storage during this period, which is assumed to be small in comparison to the total inflow or outflow for the same period. Also, this assumption does not apply if recharge to the watershed exits the watershed through deep groundwater and bypasses the stream outlet, which is possible in karst watersheds for example. Recent rainfall has the largest effect on s in Eq. (1), whereas earlier rainfall has the least effect.

The effect of changing air temperatures on daily evapotranspiration is accounted for by (Jakeman and Hornberger, 1993):

$$\kappa_i = \alpha \exp\left[(20 - T_i)f\right] \qquad f > 0, \tag{2}$$

where α [unitless] is a scaling coefficient; T [$^\circ$C] is daily mean air temperature at the land surface; and f is a temperature modulation factor [$^\circ$C^{-1}]. As air temperature T decreases, s in Eq. (1) increases with sufficient past rainfall. RRAWFLOW can be executed without air-temperature data if unavailable (air-temperature option 2 in Table 1).

Full Screen / Esc

Printer-friendly Version

Interactive Discussion

Daily recharge u_i [L] is calculated as the fraction s of daily precipitation by

$$u_i = r_i s_i. \tag{3}$$

An additional function of parameters c and κ is to adjust for differences in the runoff effects between watershed and groundwater modeling. Also, for groundwater applications, c in Eq. (1) cannot be determined empirically if the recharge area that affects a spring or well is not precisely defined. Therefore, for groundwater applications, c can be set to a value that results in a predefined maximum s value or estimated mean recharge rate, or c can be optimized through model calibration. In practice, the error in the estimation of c is compensated by an adjustment in the IRF area during model calibration; e.g., an overestimation of c by 10 % would result in a 10 % underestimation in IRF area.

Depending on the values of c and κ, the value of s can incorrectly have values < 0 or > 1; when this occurs, RRAWFLOW sets s to 0 or 1, respectively. This is most likely to occur early in the calibration process when parameter values might be far from optimum, and forcing the constraint $0 \geq s \geq 1$ assists in the efficiency of the calibration process. To ensure that the range of s is appropriate for the model area, this parameter should always be plotted after model calibration; i.e., s should be a physically plausible function that fluctuates in response to local precipitation and air temperature. For example, in humid climates with high annual precipitation, s might frequently have a value > 0.9, which is less likely in dry climates.

For cold climates where winter snowfall is common, a method proposed by Long and Maher (2013) is applied. To determine the form of precipitation for each day, an air temperature threshold value T_s is set, below which precipitation is assumed to occur as snow (typically $T_s = 0\,^{\circ}\text{C}$). To determine days when melting occurs, a melting threshold value T_m is set. If daily snow-depth data are available, T_m can be determined empirically as the mean air temperature for days when snow depth decreases to zero from a previous day with a snow depth greater than zero. Long and Mahler (2013) determined that $T_m = 9\,^{\circ}\text{C}$ for a study area in central North America. Sublimation is accounted for

by a sublimation fraction S_f. Snow precipitation is summed for each series of snow-precipitation days occurring prior to each snowmelt day by

$$p_m = (1 - S_f) \sum_{i=1}^{N} p_i \quad T_i < T_s,$$

(4)

where p_m is the accumulated snow precipitation that is assumed to melt when $T_i > T_m$, S_f is the sublimation fraction [unitless], p_i is the daily snow precipitation in height of water, and N is the number of snow precipitation days occurring between melt days. Prior to calculating Eq. (1), p_m is added to the daily rainfall record for the day following a snowmelt day because snowmelt is assumed to have the same effect as rainfall on the value of s.

2.2 Other recharge options

Recharge estimated outside of RRAWFLOW can be used as model input, in which case Eqs. (1)–(4) are not used. For example, this applies to precipitation recharge estimated by a daily soil-water-balance model (e.g., Westenbroek et al., 2010) or sinking-stream recharge in karst aquifers that can be estimated by methods such as those described by Hortness and Driscoll (1998). This is system-input option 2 (Table 1).

2.3 Solute transport

RRAWFLOW can simulate transport of a solute, similarly to the approach of Maloszewski and Zuber (1982), in which case Eqs. (1)–(4) are not used. In this case, the system input is the solute concentration, and a constant recharge rate is assumed. The response in solute concentration at the outlet of a system is simulated by the convolution integral (as described in the following section), which temporally disperses a system input of a solute. This is system-input option 3 (Table 1).

2.4 Convolution

Convolution is a time-series operation (Jenkins and Watts, 1968; Smith, 2003) commonly used in non-distributed hydrological models to simulate streamflow, springflow, or groundwater level in response to recharge (e.g., Nash, 1959; Dooge, 1973; Dreiss, 1989; Olsthoorn, 2008). The use of convolution in hydrology has its origins in unit-hydrograph theory for watershed runoff modeling (Nash, 1959; Dooge, 1973). Convolution has been used to simulate solute transport of tracers (e.g., Maloszewski and Zuber, 1982; Long and Putnam, 2004; Jurgens et al., 2012), groundwater response to recharge from a sinking stream (Long and Derickson, 1999), flow through karst conduits (Cornaton and Perrochet, 2002), and cave drip (Long and Mahler, 2013). The use of convolution in modeling also has been described as a linear-reservoir model and a transfer-function model (e.g., Nash, 1959; Young, 2013; von Asmuth et al., 2002).

Mathematically, convolution is the integration of an input function (e.g., recharge) with an IRF that describes the system response to a unit impulse of the input function:

$$y(t) = \int_{\tau=0}^{\infty} h(t - \tau)u(\tau)\mathrm{d}\tau \tag{5}$$

where $y(t)$ is the system response, or output; $h(t - \tau)$ is the IRF; $u(\tau)$ is the input, or forcing, function; τ and t are time variables corresponding to system input and output, respectively (Jenkins and Watts, 1968; Dooge, 1973; Olsthoorn, 2008). The quantity $t - \tau$ represents the delay time from impulse to response, and the IRF represents a distribution of these delay times. In RRAWFLOW, the input function $u(\tau)$ can be recharge or input of a solute. The system response $y(t)$ can be streamflow exiting a watershed, springflow from a groundwater system, groundwater level, or solute concentration at an outlet. Physically, the IRF is the system response $y(t)$ per unit impulse of $u(\tau)$ and also can be described as the response produced by a system when the input is a delta function (Smith, 2003). Conceptually, convolution is the superposition of a series of

IRFs that are initiated at the time of each impulse of $u(\tau)$ and are scaled proportionally by the magnitude of the corresponding impulse (Fig. 1).

For uniform time steps, the discrete form of Eq. (5) is

$$y_i = \sum_{j=0}^{i} h_{i-j} u_j + \varphi_i \quad i, j = 0, 1, \ldots, N, \tag{6}$$

where h_{i-j} is the IRF; u_j is the input, or forcing, function; and j and i are time-step indices corresponding to system input and output, respectively; N is the number of time steps in the output record; and φ represents the errors resulting from measurement inaccuracy, sampling interval, or simplifying model assumptions. For simulation of groundwater levels, a datum h_0 at which hydraulic head equals zero must be established. Conceptually, h_0 is the level to which hydraulic head would converge if the local recharge was eliminated. Local recharge is assumed to be the only forcing that results in hydraulic-head fluctuation or that causes hydraulic head to rise above h_0.

2.5 Impulse-response function (IRF)

The IRF also has been described by other terms, including instantaneous unit hydrograph, transfer function, and kernel (e.g., Nash, 1959; Dreiss, 1989; Berendrecht et al., 2003; Smith, 2003; Jukić and Denić-Jukić, 2006). The IRF of a hydrologic system can be approximated by a parametric function, where its shape is defined by one or more parameters, or a nonparametric function that is not constrained to common curve types. To compare convolution with frequency analysis, the frequency spectrum is a function that characterizes a single time series at a glance, whereas the IRF is a function that characterizes the relation between system input and output.

2.5.1 Parametric IRFs

Parametric functions that have been used to approximate the IRF for hydrologic systems include exponential, lognormal, and gamma functions (Nash, 1959; Besbes

and de Marsily, 1984; Jakeman and Hornberger, 1993; von Asmuth et al., 2002; Berendrecht et al., 2003; von Asmuth and Knotters, 2004; Long, 2009; Long and Mahler, 2013). The gamma function is equivalent to the Pearson type III function: the three parameters of the Pearson type III function can be combined into the two parameters of the gamma function (Haan, 2002). Estimation of parametric IRFs generally consists of model-calibration techniques to optimize the parameters with the aim of minimizing the difference between the observed and simulated system response; i.e., fitting the model. The parametric functions previously described (other than Pearson type III) have one or two of these fitting parameters. As the number of fitting parameters increases, the risk of over-fitting the model also increases; i.e., fitting the errors φ in Eq. (6).

For a parametric approximation of the IRF, RRAWFLOW uses the gamma function:

$$\gamma(t) = \frac{\lambda^\eta t^{\eta-1} e^{-\lambda t}}{\Gamma(\eta)} \quad \lambda, \eta > 0, \tag{7}$$

$$\Gamma(\eta) = \int_{t=0}^{\infty} t^{\eta-1} e^{-t} \mathrm{d}t, \tag{8}$$

where λ and η are unitless shape parameters, and the mean and variance are η/λ and η/λ^2, respectively. Equation (8) is approximated in RRAWFLOW by the discrete form

$$\Gamma(\eta) = \Delta t \sum_{t=t_0}^{N} t^{\eta-1} e^{-t}, \tag{9}$$

where t is time centered on each discrete time step; t_0 and N are time centered on the initial and final time steps, respectively; and Δt is the time step duration. The gamma function can produce a variety of shapes, including exponential ($\eta = 1$), reverse-J ($\eta < 1$), and positively skewed shapes with a peak at $t = (\eta - 1)/\lambda$ (Haan, 2002; Fig. 2). The gamma function can produce nearly identical shapes to those of the lognormal

function when $\eta > 1$, and therefore, can produce nearly all possible shapes of the exponential and lognormal functions combined when $\eta \geq 1$, plus additional shapes when $\eta < 1$. The RRAWFLOW option to use parametric IRFs is specified as IRF type 1 (Table 1).

The gamma function (Eq. 7), which has an area under its curve of unity, requires the additional scaling coefficient ε for use as the IRF in many hydrologic applications:

$$h(t) = \varepsilon \gamma(t), \tag{10}$$

where ε [unitless] compensates for hydrologic systems that do not have a one-to-one relation between system input and output (Olsthoorn, 2008). For example, if (1) the system input $u(\tau)$ is in cubic meters per day of recharge, (2) the system response $y(t)$ is springflow with the same units, and (3) 100 % of this recharge emerges as springflow with nothing else contributing to springflow, then ε would be set to unity. For most other hydrologic applications, ε would not equal unity. Similarly, if 100 % of a solute entering the system does not exit the system at the observation point, then the area under the IRF should be less than unity ($\varepsilon < 1$). Maloszewski and Zuber (1982) simulated solute transport with IRFs that were approximated by the exponential or the dispersion-model functions. The gamma function has a similar shape to that of the dispersion-model function and could be used as an approximation of the dispersion-model function, or the exact dispersion-model function can be provided to RRAWFLOW as a user-defined IRF.

RRAWFLOW allows the use of as many as two superposed gamma functions to produce additional IRF shapes (Fig. 3), herein referred to as a double-gamma IRF. Approaches similar to this have been used to represent the components of quick flow and slow flow in watershed modeling (Jakeman and Hornberger, 1993) and for conduit and diffuse flow in karst aquifers (Pinault et al., 2001; Long, 2009; Long and Mahler, 2013). In these examples, each parametric function represents one of two flow components. The use of a double-gamma IRF also might be useful when a single function cannot produce the necessary IRF approximation (e.g., an extra-long tail). The scaling

coefficient ε can be set to different values for the two gamma functions; e.g., to allow for a larger component of slow flow than quick flow.

2.5.2 Nonparametric IRFs

The process of determining an unknown IRF from observed system input and output data is known as deconvolution (e.g., Neuman and de Marsily, 1976). To define a nonparametric IRF, an ordinate value is defined for each time step, and any shape desired is possible. Deconvolution methods include Fourier harmonic time-series analysis (Blank et al., 1971; Delleur and Rao, 1971), linear programming (Neuman and de Marsily, 1976), and time-moment analysis (Dreiss, 1989). Estimations of nonparametric IRFs by model calibration include those described by Pinault et al. (2001), Jukić and Denić-Jukić (2006), and Long and Mahler (2013). A potential problem with nonparametric IRFs is that hundreds or even thousands of IRF ordinates may be needed to define the IRF, depending on the IRF length and time step. Optimization of each individual ordinate would result in a mathematically underconstrained and over-fit model. An extreme example of over-fitting is to determine the IRF by means of deconvolution in the frequency domain (Smith, 2003) that results in a numerically perfect model fit but also an IRF that commonly is highly oscillatory and cannot be explained physically (Blank et al., 1971; and Delleur and Rao, 1971) because the errors φ (Eq. 6) are included in the fitting process. Further, an over-fitted model results in a poor model fit when tested on a conditional validation period that was sequestered from the fitting process. Pinault et al. (2001), Jukić and Denić-Jukić (2006), and Ladouche et al. (2014) described different methods to constrain the nonparametric IRF and reduce the number of fitting parameters.

The method proposed herein uses a small number of ordinates to define a smoothly shaped nonparametric IRF: ordinates of the IRF are defined at spaced intervals (IRF control points), and a spline curve is fit through these points (Fig. 4) (IRF type 2, Table 1). Another option is to apply straight-line segments connecting the control points (IRF type 3, Table 1). Similar to parametric IRFs, these two nonparametric options are

convenient for the estimation of the IRF through model calibration and conditional validation because of the ability to control the number of fitting ordinates. If a model is suspected of having been over-fit, the number of control points should be reduced; this consists of increasing the control-point intervals, resulting in a smoother shape, or by reducing the tail length by setting posterior control points to zero. Another option allows a predefined IRF to be supplied to RRAWFLOW if the IRF is determined by some other method (IRF type 4, Table 1). The scaling coefficient ε is not necessary for nonparametric IRFs because the area is defined by the ordinate values.

2.5.3 System linearity

Estimated recharge (Eqs. 1–4) is a nonlinear process, where the daily fraction of precipitation varies with antecedent soil-moisture conditions. Convolution (Eq. 5), which simulates the system response to recharge, is a linear process (Jenkins and Watts, 1968; Dooge, 1973); this is consistent with Jakeman and Hornberger (1993), who described the response of streamflow to recharge as predominantly a linear process for a variety of watersheds of differing size.

A linear system can be either time variant or time invariant, depending on whether or not the IRF changes with time (Jenkins and Watts, 1968). Most commonly, a time-invariant (i.e., static) IRF is assumed in hydrological convolution models (e.g., von Asmuth et al., 2002; Denić-Jukić and Jukić, 2003). In many hydrological systems, however, the IRF changes with changing hydrological conditions, resulting in a change in the flow system. For example, an increase in groundwater hydraulic gradient generally results in an increase in groundwater velocity. Fluctuating groundwater levels might saturate or desaturate different parts of the aquifer having different hydraulic-conductivity values or, in karst aquifers, different conduit or fracture networks. Examples of time-variant IRFs for karst applications include Pinault et al. (2001), Jukić and Denić-Jukić (2006), and Long and Mahler (2013).

2.5.4 Time variance

RRAWFLOW has three options for time variance in convolution (Table 1). In time-variance (TV) option 1, the IRF is time invariant, or static. TV option 2 applies a time-variant IRF, similarly to the method proposed by Long and Mahler (2013), which uses a minimal number of fitting parameters but also represents the dominant transient characteristics of the system. In this method, the system input record is separated into climatically wet or dry periods; e.g., months or years for which the mean precipitation is either above or below the long-term mean, respectively. One IRF represents all of the wet periods, and the other represents all of the dry periods. This is applicable when different altitudes of the groundwater table result in different hydraulic gradients (e.g., toward a stream) or the saturation of different subterranean features with different hydraulic characteristics. Larocque et al. (1998), for example, observed that high-flow and low-flow periods could be identified by distinct hydraulic characteristics for a karst aquifer in France.

All of the parametric and nonparametric IRF-type options previously described can be used in TV option 2 (Table 1). An advantage of this method is that both the size and shape of the IRF can change, while the fitting parameters are kept to a minimum because IRFs are not defined continuously but rather for two different periods only. A potential disadvantage of this method is that the IRF changes abruptly between wet and dry periods; however, this was not a detrimental factor for several models in which this method was applied (Long and Mahler, 2013). Also, the superposition of many responses applied in convolution results in smooth transitions in the simulated response between wet and dry periods, even with different IRFs for the two periods. Jukić and Denić-Jukić (2006) proposed a similar time-variant approach, where three different IRFs each were applied to one of three different hydrological periods determined by an index of antecedent recharge.

Pinault et al. (2001) varied the IRF's vertical scale continuously with hydraulic head. However, because hydraulic head also is used for model calibration, this

approach cannot be used to simulate periods without observed system-response data; e.g., future periods that might be simulated with climate projections. TV option 3 in RRAWFLOW (Table 1) is similar to the approach of Pinault et al. (2001), except that the IRF scale varies according to the input for convolution $u(\tau)$ (e.g. recharge), and the variable β is inserted into Eq. (6), resulting in

$$y_i = \Delta t \sum_{j=0}^{i} \beta_j h_{i-j} u_j + \phi_i \quad i = 0, 1, \ldots, N \tag{11}$$

$$\beta_j = m x_j \quad m \neq 0 \tag{12}$$

where x is the moving average of $u(\tau)$ that is scaled to range from 0 to 1, and m determines the range of β. A moving average of $u(\tau)$ is used so that the IRF transitions smoothly. Generally, β is assumed to vary directly with x ($m > 0$). Advantages of this method are that it requires fewer fitting parameters than TV option 2 and the IRF does not change abruptly; the disadvantage is that only the vertical scale of the IRF changes, whereas the shape is static. All of the parametric and nonparametric IRF-type options previously described can be used in this option. TV option 3 has longer run times than TV options 1 or 2 because of the additional computation required, mainly within the convolution loop.

For time-invariant systems, the cross-correlation function (CCF) has the same shape as the IRF but only if the input to the convolution process is completely random (Jenkins and Watts, 1968). If the convolution input has a strong autocorrelation, typical of recharge in hydrological systems, then there is large error in using the CCF to estimate the IRF (Jenkins and Watts, 1968; Bailly-Comte et al., 2011) and therefore should be avoided.

2.6 Model outputs

Model outputs consist of time series for simulated system response $y(t)$, the dry-period and wet-period IRFs, the soil-moisture index s, and the input to convolution $u(\tau)$. Other

outputs consist of a coefficient of efficiency E to measure the similarity between simulated and observed system response (residuals) and the hydrological memory of the system. This system memory is the time that the response to an impulse effectively persists, which is defined by the length of the IRF. Because the gamma function is asymptotic and has infinite length, system memory is defined in RRAWFLOW as time t_m on the IRF time scale at which 95 % of the curve area is in the range 0–t_m.

2.7 Evaluating model fit and over-fitting

The calibration period is the period of the data record used to calibrate the model. By default in RRAWFLOW, the conditional validation period is the part of the data record following the calibration period that is used to test the model calibration against system-response observation data not used in calibration (i.e., model prediction of streamflow or springflow). Assessing the conditional validation period is an indication of the expected model performance to predict a future period on the basis of climate simulations, for example; this assessment also indicates if the model is being over-fit. This validation is considered conditional because the model cannot yet be tested against additional observational data that will be available in the future (Beven and Young, 2013). RRAWFLOW calculates the Nash–Sutcliffe coefficient of efficiency (Nash and Sutcliffe, 1970; Legates and McCabe, 1999) to quantify model fit. The coefficient of efficiency E is defined as

$$E = 1 - \left[\frac{\sum (y_{\text{obs}} - y_{\text{sim}})^2}{\sum (y_{\text{obs}} - y_{\text{mean}})^2} \right], \tag{13}$$

where y_{obs} and y_{sim} are daily time series of the observed and simulated system responses, respectively, and y_{mean} is the mean value of y_{obs}. Conceptually, E is the ratio of the magnitude of model residuals (numerator) to the overall variability in the observation record (denominator) subtracted from unity and theoretically can vary from $-\infty$ (poorest fit) to unity (perfect fit). An E value of zero indicates that the observed mean

(y_{mean}) is an equally good predictor as is the simulation (y_{sim}) (Legates and McCabe, 1999). Because E compares the residuals to the overall response variability, E values for different simulated sites can be directly compared; this would not be true if the magnitude of the residuals alone is used in comparisons; e.g., as with the root mean square error.

In addition to quantifying model fit, the coefficient of efficiency provides a useful way to evaluate possible over-fitting of the model. Although model fit for the calibration period might improve as parameters are added, if the validation period indicates that this added complexity is not helpful, the model has been over-fit (von Asmuth et al., 2002). To test this condition, E is calculated for the calibration and conditional validation periods separately (E_{cal} and E_{val}). For direct comparison of E_{cal} and E_{val}, the denominator must be consistent for both cases, and therefore, the denominator is calculated on the basis of the total period and the numerator on the basis of the shorter period of interest (Long and Mahler, 2013). The denominator of Eq. (13) is scaled down to be consistent with the time period of the numerator:

$$E = 1 - \frac{\left[\sum (y_{obs} - y_{sim})^2\right]_p}{\left[\sum (y_{obs} - y_{mean})^2\right]_T (l_p/l_T)},$$

where the subscript p refers to the partial period, either calibration or conditional validation, the subscript T refers the total period, and l is the time length of the respective period. This method is particularly important for comparison of two periods with different fluctuation amplitudes. For the total period, E is calculated by Eq. (13), which is equivalent to using Eq. (14) because the partial and total periods are equal. Therefore E, E_{cal}, and E_{val} all are directly comparable.

Generally, E_{cal} will be larger (better fit) than E_{val}, but a large difference indicates possible over-fitting, in which case a simpler model (i.e., fewer fitting parameters) should be tested. For example, if a double-gamma IRF is used, then a second model calibration with a single-gamma IRF could be tested to determine if greater similarity in the

Back | Close

Full Screen / Esc

Printer-friendly Version

Interactive Discussion

E_{val} and E_{cal} values is achieved. For nonparametric IRFs, a reduction in the number of IRF control points could be tested. A time-variant IRF requires more parameters than a time-invariant IRF, and this also can be tested. Thoroughly considering model complexity in light of E_{val} and E_{cal} provides context for conditional validation. For example,
Long and Mahler (2013) described decision criteria to evaluate model complexity and the number of fitting parameters on the basis of E_{cal} and E_{val}, with several examples of calibrated models.

Numerous other researchers have investigated issues related to model complexity and its effect on model-prediction uncertainty (e.g., Jakeman and Hornberger, 1993; Arkesteijn and Pande, 2013; Pande et al., 2014). Prediction uncertainty crucially depends on model complexity (Arkesteijn and Pande, 2013). Although Vapnik–Chervonenkis generalization theory suggests that models with higher complexity tend to have higher prediction uncertainty, model complexity is not necessarily related to the number of parameters (Fienen et al., 2010; Pande et al., 2014). Although a rigorous assessment of prediction uncertainty is beyond the scope of this study, effective tools are available for this purpose (Doherty, 2005; Fienen et al., 2010).

3   Example model applications

The model was applied to two hydrological systems in the United States with responses of springflow and groundwater level. Several examples with different RRAWFLOW options and different levels of parameterization are described, including examples of model over-fitting. Model input data consisting of daily precipitation and air temperature and system-response observation data used for model evaluation are described in Long and Mahler (2013) along with details describing the hydrogeology, physiography, and climate of these sites. The precipitation records were separated into wet and dry periods, which were defined as years in which the annual precipitation was either above or below the long-term mean, respectively.

Model spin-up is the initial simulation period in which antecedent effects of the system are not fully incorporated into the simulation, and therefore, model output for this period is not valid. When the simulation is past the number of time steps equal to the system memory, then the system antecedent effects are fully incorporated into the model. Therefore, the model input record must start n time steps prior to the calibration period, where n is the system memory as a number of time steps. Because the system memory is not known until the IRF is estimated, it is useful to start the simulation at the earliest date for which input data are available. Estimated system-input values can be used if observation data are not available for this antecedent-period requirement, and a constant value equal to the long-term mean can be used if a better estimate is not available; in this case, the antecedent effects will be smoothed.

The parameter optimization software PEST (Doherty, 2005) was used for parameter estimation. For optimization of nonparametric IRFs, the last control point was used to set the system memory by assigning a fixed (non-optimized) value of zero to that control point (Fig. 4). Posterior to this point, a series of control points fixed at zero was specified, resulting in a spline fit with a constant value of zero.

3.1 Springflow from Barton Springs

Barton Springs is a group of springs that flow from the Edwards aquifer, a carbonate aquifer in south-central Texas that is contained mostly within the Edwards Group (Lower Cretaceous geologic age). The collective flow from these springs was simulated in these examples. The springs respond to surface recharge to the Edwards aquifer that occurs from multiple sinking streams that cross onto the aquifer's recharge area and precipitation recharge (Mahler et al., 2008). The example models described used system-input option 1 (precipitation recharge, Table 1). Although recharge for Barton Springs also includes sinking-stream recharge, option 1 provided an approximation of total recharge. Seven example models are presented for Barton Springs (Table 2). These examples also serve to describe model settings for simulation of streamflow, because the model settings for springflow and streamflow are identical. Generally, E_cal

is proportional to the number of optimized parameters for each example; however, high E_{cal} values often result in low values of E_{val}, which might indicate over fitting (Table 2). Therefore, the type of model applied and the number of parameters needed for the selected model are important considerations. Table 3 shows parameters for single-gamma and double-gamma IRFs for selected example models.

Example N1 used TV option 1 (time-invariant IRF, Table 1) with a single-gamma IRF, resulting in E_{cal} and E_{val} values of 0.84 and 0.63 (Table 2); as is common, E_{cal} is larger than E_{val} because the validation period was not used in calibration.

Examples F5–F9 used TV option 2, in which time variance is applied as different IRFs for wet and dry periods. Example F5 used single-gamma IRFs (Figs. 5 and 6), resulting in E_{cal} and E_{val} values of 0.88 and 0.72, respectively (Table 2), which represent an improvement in model fit compared to example N1. Example F7 used double-gamma IRFs (Fig. 7), resulting in E_{cal} and E_{val} values of 0.90 and 0.63, respectively (Table 2); the added parameters for this example resulted in a higher E_{cal} value but a lower E_{val} value than for example F5, indicating that example F5 is the better choice for hydrologic projections and that example F7 was over-fit. Example F8 used nonparametric IRFs with a spline curve fit to 4 and 3 optimized (non-zero) control points for the wet and dry periods, respectively (Fig. 8a; $E_{cal} = 0.88$, $E_{val} = 0.72$), which is the same model fit as for example F5. Example F9 is the same as example F8, except with 8 optimized control points for each of the two periods (Fig. 9), which resulted in a higher E_{cal} (0.92) but a much lower E_{val} (0.61) than for example F8, indicating an over-fit model. Of the time-variant examples F5–F9, the two examples with the smallest number of optimized parameters (F5 and F8) had the largest E_{val} values (Table 2).

Examples N2 and N3 used TV option 3, in which a time-variant IRF that changes continually, with a single-gamma IRF and moving-average (MA) windows of 1 and 10 years (Eq. 12), respectively. For these examples, E_{cal} and E_{val} values were equal to or smaller than all other time-variant examples (Table 2). Increasing the MA window from 1 to 10 years improved E_{cal} and E_{val} values; this, and the fact that the wet and dry periods defined for examples F5–F9 generally are multi-year periods, indicates that the

time-variant aspects of this system respond to general climatic changes over decadal periods more so than annual.

PEST was used to calculate 95 % confidence intervals for the optimized parameters, as described in Doherty (2005), which are shown graphically for example F8 (Fig. 8b). Example F9, with a total of 16 control points, has 32 % wider parameter confidence intervals than does example F8, with 7 control points. Confidence intervals generally widen with an increasing number of parameters because of a decrease in individual parameter sensitivity.

Examples F5 and F8 are the two preferred models for Barton Springs and are nearly identical in terms of E_{val} and the number of optimized parameters (Table 2). Choosing between these two models, therefore, might be a matter of modeler preference. Use of the gamma function (example F5) has the advantage of being a common function. The control-points method (example F8) has the advantage that confidence intervals for the IRF can be easily shown in a graph (Figs. 8 and 9). Showing confidence intervals for a gamma function also could be done but with additional steps involved, in which the gamma function would have to be calculated for all combinations of the 95 % parameter confidence intervals. Then this family of curves would be plotted, and the maximum upper and lower curve extents would show the confidence intervals for the IRF. A disadvantage of the control-points method is the need to select the temporal locations of control points and also to set the system memory a priori by setting a zero-value control point at the end of the IRF. These settings generally require trial and error.

3.2 Groundwater level in well LA88C

Well LA88C, located in western South Dakota, is open to the Madison aquifer that is composed of limestone and dolostone and is contained within the regionally extensive Madison Limestone of Mississippian geologic age. This formation is exposed at the land surface on all flanks of the Black Hills of South Dakota and Wyoming and dips radially outward in all directions below the land surface. Water level in the well responds to surface recharge to the Madison aquifer that occurs from direct precipitation

and sinking streams that cross onto the aquifer's recharge area (Carter et al., 2001). The example models described used system-input option 1 (precipitation recharge, Table 1).

Examples F10–F13 apply to well LA88C and used TV option 2 for time variance (Table 1). As with Barton Springs, all E_{cal} values were larger than E_{val} (Table 2). Example F10 used double-gamma IRFs (Figs. 10 and 11; $E_{cal} = 0.92$, $E_{val} = 0.73$). Example F12 used nonparametric IRFs with spline curves fit to 10 and 8 optimized control points for the wet and dry periods, respectively (Fig. 12; $E_{cal} = 0.93$, $E_{val} = 0.70$). In example F12, the last two control points for the wet period and the last control point for the dry period were optimized to zero, resulting in only 15 non-zero control points. Example F13 used nonparametric IRFs with spline curves fit to 5 optimized control points for each of the two periods (Fig. 13; $E_{cal} = 0.88$, $E_{val} = 0.75$), resulting in a higher E_{val} value than for example F12, which indicates that the smaller number of control points is the better choice in this case. Of the three examples for well LA88C, example F13 had the fewest optimized IRF parameters and resulted in the largest E_{val} value (Table 2), indicating that example F13 is the clearly the best choice. Example F13 also resulted in the smallest E_{cal} value of the three examples, which is not a disadvantage when the primary objective is to conditionally validate the model. IRFs for example F13 approach zero abruptly, resulting in negative values in the spline curve (Fig. 13); in these cases, RRAWFLOW sets all negative values to zero.

4 Discussion and conclusions

Additional functionality can be added to RRAWFLOW by the user and could possibly be included in future versions. For example, additional methods to estimate parametric or nonparametric IRFs (e.g., the dispersion-model IRF) or the degree-day method for estimating snowmelt (Rango and Martinec, 1995) could be added. If there were a need to include precipitation recharge and sinking-stream recharge simultaneously in one system, this could easily be added. Revisions, additions, and corrections to the

Full Screen / Esc

RRAWFLOW code can be sent to the author of this article for incorporation into subsequent official versions.

Comparison of the Nash coefficient of efficiency E (measure of model fit) for calibration (E_{cal}) and conditional validation (E_{val}) periods is useful for assessing over-fitting. If E_{cal} is much larger than E_{val}, then the model may have been over-fit. Examples of model over-fitting (i.e., too many fitting parameters) include using a double-gamma IRF when a single-gamma IRF is suitable, applying time-variant IRFs when time invariance is adequate, or using more control points for a spline fit than necessary. Generally, the objective should be to maximize E_{val} to achieve the best conditional validation possible, which frequently is at the expense of lowering E_{cal}. The selection of IRF type, number of control points, and time-variance options to maximize E_{val} can be done by testing multiple options. Too many fitting parameters, as well as too few, can result in low values of E_{val}.

The record length of the observed response should be considered in light of the system memory: there is less confidence in the predictive strength of a model if the observed response is shorter than the system memory than if it is longer, because, in the former case, the effects of the IRF tail are not fully tested against observation. Ideally, the validation period alone should be longer than the system memory, and if it is several times longer, then the full range of the IRF is tested several times over.

RRAWFLOW is suitable for hydrograph-separation methods to estimate stream base-flow, as described by Jakeman and Hornberger (1993) and Long (2009). IRFs for streamflow commonly have a slow-flow component with a much smaller peak response and much longer tail than the quick-flow component, as in Fig. 3. For the simulated hydrograph, RRAWFLOW can be used to compute the base-flow component by executing the model without the quick-flow IRF. To estimate the base-flow component of the observed hydrograph, a graphical separation program can be used, such as PART (Rutledge, 1998); however, because the different options and settings in PART (or similar programs) result in different base-flow estimates, the RRAWFLOW estimated base flow is helpful as guide to using PART (Long, 2009). For example, the PART settings

can be adjusted so that the observed hydrograph separation has similar characteristics to those of the simulated hydrograph separation.

Code availability

The RRAWFLOW program written in R language, RRAWFLOW manual, and an example model are included in the Supplement to this article. The model included is example F5 for Barton Springs previously described (Table 2). It is not necessary to know the R language to execute the model, but R must be installed on the user's computer. The example is set up to run on the Microsoft[®] Windows operating system but could be slightly modified to run on a Linux operating system. No license is needed for RRAWFLOW.

The example model is set up for parameter optimization using the PEST software program (Doherty, 2005) for model calibration. All RRAWFLOW input and output files are included along with PEST input, output, and executable files. The file 00_ReadMe.pdf in the Supplement contains instructions for executing RRAWFLOW in the R environment and basic instructions for PEST exectution for this example. The RRAWFLOW manual has detailed input and output instructions, and additional details for using PEST are in Doherty (2005). The Supplement can be used as a template for a new modeling project by editing the input files accordingly. The R language program and PEST can be downloaded at no cost from http://www.r-project.org/index.html and http://www.pesthomepage.org/, respectively. Tables S1–S4 in the Supplement contain model input values for all examples previously described.

The Supplement related to this article is available online at doi:10.5194/gmdd-7-5919-2014-supplement.

References

Arkesteijn, L. and Pande, S.: On hydrological model complexity, its geometrical interpretations and prediction uncertainty, Water Resour. Res., 49, 7048–7063, 2013.

Bailly-Comte, V., Martin, J. B., and Screaton, E. J.: Time variant cross correlation to assess residence time of water and implication for hydraulics of a sink-rise karst system, Water Resour. Res., 47, W05547, doi:10.1029/2010WR009613, 2011.

Berendrecht, W. L., Heemink, A. W., Van Geer, F. C., and Gehrels, J. C.: Decoupling of modeling and measuring interval in groundwater time series analysis based on response characteristics, J. Hydrol., 278, 1–16, 2003.

Besbes, M. and de Marsily, G.: From infiltration to recharge: use of a parametric transfer function, J. Hydrol., 74, 271–293, 1984.

Beven, K.: Changing ideas in hydrology – The case of physically-based models, J. Hydrol., 105, 157–172, 1989.

Beven, K. and Young, P.: A guide to good practice in modeling semantics for authors and referees, Water Resour. Res., 49, 5092–5098, 2013.

Blank, D., Delleur, J. W., and Giorgini, A.: Oscillatory kernel functions in linear hydrologic models, Water Resour. Res., 7, 1102–1117, 1971.

Carter, J. M., Driscoll, D. G., and Hamade, G. R.: Estimated recharge to the Madison and Minnelusa aquifers in the Black Hills area, South Dakota and Wyoming, water years 1931–98, US Geol. Surv., Reston Virginia, Water-Resources Investigations Report 00-4278, 66 pp., 2001.

Cornaton, F. and Perrochet, P.: Analytical 1D dual-porosity equivalent solutions to 3D discrete single-continuum models. Application to karstic spring hydrograph modelling, J. Hydrol., 262, 165–176, 2002.

Delleur, J. W. and Rao, R. A.: Linear systems analysis in hydrology: the transform approach, kernel oscillations and the effect of noise, in: Systems Approach to Hydrology, Water Resources Publications, Fort Collins, Colorado, 116–142, 1971.

Denić-Jukić, V. and Jukić, D.: Composite transfer functions for karst aquifers, J. Hydrol., 274, 80–94, 2003.

Doherty, J.: PEST – Model-Independent Parameter Estimation, User Manual (5th Edn.), Watermark Numerical Computing, Brisbane, Australia, available at: http://www.pesthomepage.org/ (last access: 3 September 2014), 2005.

Dooge, J. C. I.: Linear theory of hydrologic systems, Washington, D.C., 1468 pp., 1973.

Dreiss, S. J.: Regional scale transport in a karst aquifer: 2. Linear systems and time moment analysis, Water Resour. Res., 25, 126–134, 1989.

Fienen, M. N., Doherty, J. E., Hunt, R. J., and Reeves, H. W.: Using prediction uncertainty analysis to design hydrologic monitoring networks: example applications from the Great Lakes water availability pilot project, US Geol. Surv., Reston Virginia, Scientific Investigations Report 2010–5159, 44 pp., 2010.

Haan, C. T.: Statistical Methods in Hydrology, 2nd Edn., The Iowa State University Press, Ames, Iowa, 2002.

Hortness, J. E. and Driscoll, D. G.: Streamflow losses in the Black Hills of western South Dakota, US Geol. Surv., Reston Virginia, Water-Resources Investigations Report 98-4116, 99 pp., 1998.

Jakeman, A. J. and Hornberger, G. M.: How much complexity is warranted in a rainfall-runoff model?, Water Resour. Res., 29, 2637–2649, 1993.

Jenkins, G. M. and Watts, D. G.: Spectral Analysis and its Applications, Holden-Day, San Francisco, California, 1968.

Jukić, D. and Denić-Jukić, V.: Nonlinear kernel functions for karst aquifers, J. Hydrol., 328, 360–374, 2006.

Jurgens, B. C., Bohlke, J. K., and Eberts, S. M.: TracerLPM (Version 1): An Excel® workbook for interpreting groundwater age distributions from environmental tracer data, US Geological Survey, Reston, VA, Techniques and Methods Report 4-F3, 60 pp., 2012.

Ladouche, B., Marechal, J., and Dorfliger, N.: Semi-distributed lumped model of a karst system under active management, J. Hydrol., 509, 215–230, 2014.

Larocque, M., Mangin, A., Razack, M., and Banton, O.: Contribution of correlation and spectral analyses to the regional study of a large karst aquifer (Charente, France), J. Hydrol., 205, 217–231, 1998.

Legates, D. R. and McCabe Jr., G. J.: Evaluating the use of "goodness-of-fit" measures in hydrologic and hydroclimatic model validation, Water Resour. Res., 35, 233–241, 1999.

Long, A. J.: Hydrograph separation for karst watersheds using a two-domain rainfall-discharge model, J. Hydrol., 364, 249–256, 2009.

Long, A. J. and Derickson, R. G.: Linear systems analysis in a karst aquifer, J. Hydrol., 219, 206–217, 1999.

Long, A. J. and Mahler, B. J.: Prediction, time variance, and classification of hydraulic response to recharge in two karst aquifers, Hydrol. Earth Syst. Sci., 17, 281–294, doi:10.5194/hess-17-281-2013, 2013.

Long, A. J. and Putnam, L. D.: Linear model describing three components of flow in karst aquifers using ^{18}O data, J. Hydrol., 296, 254–270, 2004.

Mahler, B. J., Valdes, D., Musgrove, M., and Massei, N.: Nutrient dynamics as indicators of karst processes: Comparison of the Chalk aquifer (Normandy, France) and the Edwards aquifer (Texas, U.S.A.), J. Contam. Hydrol., 98, 36–49, 2008.

Maloszewski, P. and Zuber, A.: Determining the turnover time of groundwater systems with the aid of environmental tracers. 1. Models and their applicability, J. Hydrol., 57, 207–231, 1982.

Nash, J. E.: Systematic determination of unit hydrograph parameters, J. Geophys. Res., 54, 111–115, 1959.

Nash, J. E. and Sutcliffe, J. V.: River flow forecasting through conceptual models part I – A discussion of principles, J. Hydrol., 10, 282–290, 1970.

Neuman, S. P. and de Marsily, G.: Identification of linear systems response by parametric programming, Water Resour. Res., 12, 253–262, 1976.

Olsthoorn, T. N.: Do a bit more with convolution, Ground Water, 46, 13–22, 2008.

Pande, S., Arkesteijn, L., Savenije, H. H. G., and Bastidas, L. A.: Hydrological model parameter dimensionality is a weak measure of prediction uncertainty, Hydrol. Earth Syst. Sci. Discuss., 11, 2555–2582, doi:10.5194/hessd-11-2555-2014, 2014.

Pinault, J. L., Plagnes, V., Aquilina, L., and Bakalowicz, M.: Inverse modeling of the hydrological and the hydrochemical behavior of hydrosystems; characterization of karst system functioning, Water Resour. Res., 37, 2191–2204, 2001.

Title Page

Abstract | Introduction

Conclusions | References

Tables | Figures

Back | Close

Full Screen / Esc

Printer-friendly Version

Interactive Discussion

Rango, A. and Martinec, J.: Revisiting the degree-day method for snowmelt computations, Water Resour. Bull., 31, 657–669, 1995.

Reed, S., Koren, V., Smith, M., Zhang, Z., Moreda, F., and Seo, D.-J.: Overall distributed model intercomparison project results, J. Hydrol., 298, 27–60, 2004.

Rutledge, A. T.: Computer programs for describing the recession of ground-water discharge and for estimating mean ground-water recharge and discharge from streamflow records-update, US Geol. Surv., Reston Virginia, Water-Resources Investigations Report 98-4148, 52 pp., 1998.

Smith, S. W.: Digital Signal Processing: A Practical Guide for Engineers and Scientists, Newnes, Amsterdam, 2003.

Smith, M., Koren, V., Zhang, Z., Moreda, F., Cui, Z., Cosgrove, B., Mizukami, N., Kitzmiller, D., Ding, F., Reed, S., Anderson, E., Schaake, J., Zhang, Y., Andréassian, V., Perrin, C., Coron, L., Valéry, A., Khakbaz, B., Sorooshian, S., Behrangi, A., Imam, B., Hsu, K.-L., Todini, E., Coccia, G., Mazzetti, C., Ortiz Andres, E., Francés, F., Orozco, I., Hartman, R., Henkel, A., Fickenscher, P., and Staggs, S.: The distributed model intercomparison project – Phase 2: Experiment design and summary results of the western basin experiments, J. Hydrol., 507, 300–329, 2013.

Symstad, A. J., Long, A. J., Stamm, J. F., King, D. A., and Bachelet, D. M.: Two Approaches for Planning Natural Resource Management in a Changing Climate at Wind Cave National Park, National Park Service Natural Resource Technical Report NPS/WICA/NRTR—2014/XXX, 81 pp., in review, 2014.

von Asmuth, J. R. and Knotters, M.: Characterising groundwater dynamics based on a system identification approach, J. Hydrol., 296, 118–134, 2004.

von Asmuth, J. R., Bierkens, M. F. P., and Maas, K.: Transfer function-noise modeling in continuous time using predefined impulse response functions, Water Resour. Res., 38, 1287, doi:10.1029/2001WR001136, 2002.

Westenbroek, S. M., Kelson, V. A., Dripps, W. R., Hunt, R. J., and Bradbury, K. R.: SWB – A modified Thornthwaite-Mather soil-water-balance code for estimating groundwater recharge, US Geol. Surv., Reston Virginia, Techniques and Methods 6-A31, 60 pp., 2010.

Young, P. C.: Hypothetico-inductive data-based mechanistic modeling of hydrological systems, Water Resour. Res., 49, 915–935, 2013.

Table 1. RRAWFLOW options.

System input
1 = System input is precipitation that results in recharge to the system (Eqs. 1–4).
2 = System input is recharge estimated outside of RRAWFLOW (skip Eqs. 1–4).
3 = System input is solute concentration (skip Eqs. 1–4).

System output
1 = System output is groundwater level.
2 = System output is springflow or streamflow.
3 = System output is solute concentration (System input = 3).

IRF type
1 = Parametric IRF – gamma functions.
2 = Nonparametric IRF – spline fit to IRF control points.
3 = Nonparametric IRF – linear fit to IRF control points.
4 = Nonparametric IRF – user-defined IRF.

Time variance (TV) in convolution
1 = Time-invariant (static) IRF.
2 = Wet-period IRF and dry-period IRF are defined separately, and each are time invariant within these respective periods.
3 = Variable IRF vertical scale, where β in Eq. (11) is variable.

Air temperature
1 = Use air temperature adjustment (Eq. 2).
2 = Do not use air temperature adjustment.

Table 2. Summary of example models. The rows in italic font indicate the best choices.

Site	Example	Figure	Time-variance (TM) option	Description of impulse-response function (IRF)	No. of optimized IRF parameters	Time variant	E_{cal}	E_{val}	Comments
Barton Springs	N1	–	1	Single-gamma IRF (static)	3	no	0.84	0.63	Poor E_{val}
	F5	*5*	*2*	*Single-gamma IRFs*	*6*	*yes*	*0.88*	*0.72*	*Good E_{val}*
	F7	7	2	Double-gamma IRFs	12	yes	0.90	0.63	Over fit
	F8	*8*	*2*	*7 optimized control points*	*7*	*yes*	*0.88*	*0.72*	*Good E_{val}*
	F9	9	2	16 optimized control points	16	yes	0.92	0.61	Over fit
	N2	–	3	Single-gamma, variable-scale IRF; 1-year window	4	yes	0.80	0.46	PoorE_{val}
	N3	–	3	Single-gamma, variable-scale IRF; 10-year window	4	yes	0.84	0.61	PoorE_{val}
Well LA88C	F10	10	2	Double-gamma IRFs	12	yes	0.92	0.73	–
	F12	12	2	18 optimized control points	18	yes	0.93	0.70	–
	F13	*13*	*2*	*10 optimized control points*	*10*	*yes*	*0.88*	*0.75*	*Best E_{val} and smallest number of parameters*

Table 3. Impulse-response function (IRF) parameters for selected example models.

Example	F5	F7	F10
Site	Barton Springs	Barton Springs	Well LA88C
IRF type	Single-gamma IRFs	Double-gamma IRFs	Double-gamma IRFs
Dry period			
λ_1	2.15×10^{-4}	5.26×10^{-4}	5.15×10^{-3}
η_1	6.26×10^{-1}	6.61×10^{-1}	1.15×10^{0}
ε_1	2.01×10^{1}	1.65×10^{1}	1.08×10^{2}
λ_2	0	3.82×10^{-2}	1.31×10^{-2}
η_2	0	5.10×10^{1}	6.36×10^{0}
ε_2	0	4.98×10^{0}	1.42×10^{2}
Wet period			
λ_3	6.39×10^{-3}	7.77×10^{-3}	1.57×10^{-3}
η_3	1.14×10^{0}	1.22×10^{0}	1.16×10^{0}
ε_3	1.09×10^{1}	1.11×10^{1}	2.50×10^{2}
λ_4	0	9.53×10^{-2}	1.89×10^{-2}
η_4	0	4.95×10^{1}	3.86×10^{1}
ε_4	0	8.03×10^{-1}	5.28×10^{1}
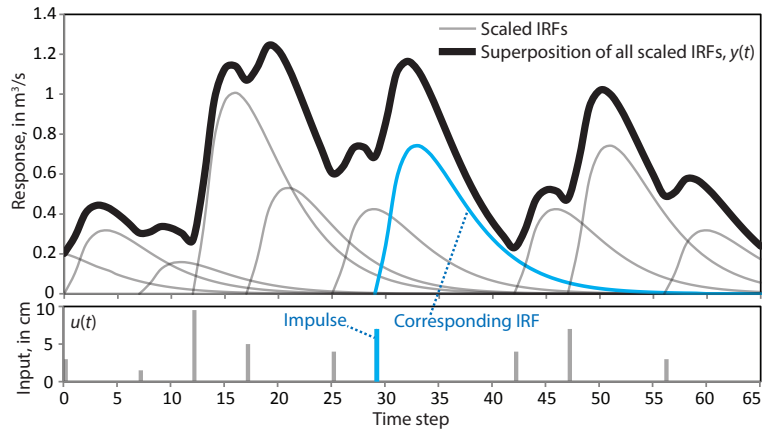
Figure 1. Superposition of sequential impulse-response functions (IRFs). Each IRF is in response to an impulse of the input function $u(\tau)$ and is scaled by the magnitude of that impulse.

Full Screen / Esc

Printer-friendly Version

Interactive Discussion
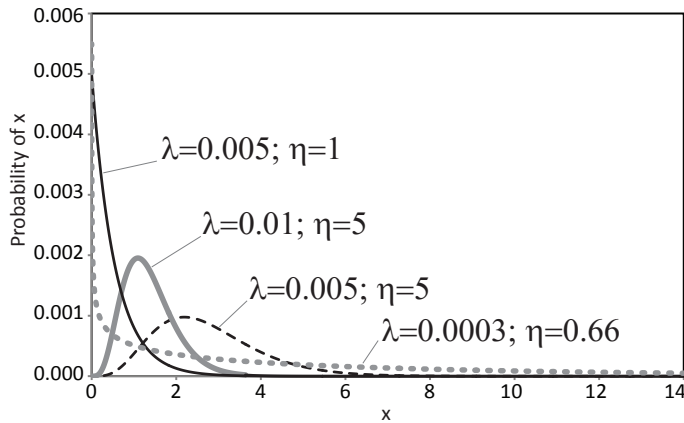
Figure 2. Gamma functions for different values of its two shape parameters.
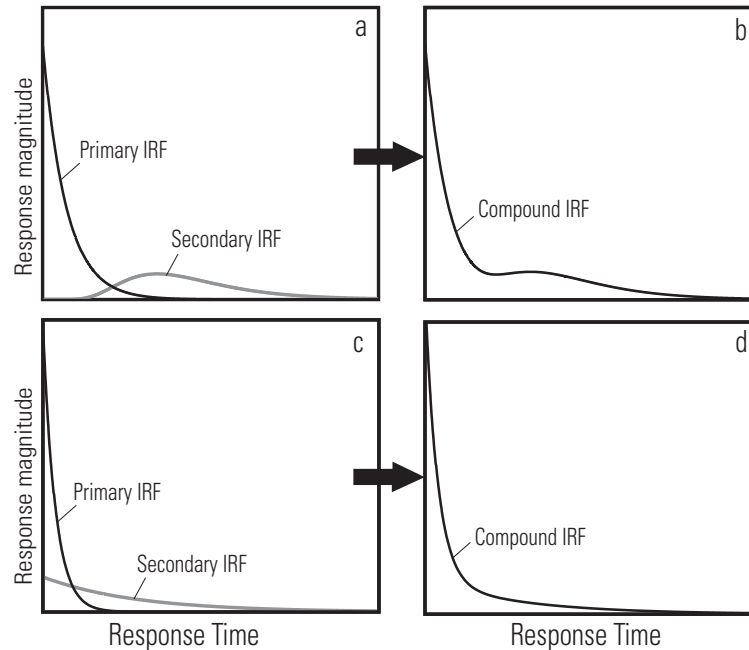
Figure 3. Superposition of two gamma functions to produce different impulse-response function (IRF) shapes. In some cases, this double-gamma IRF represents quick-flow and slow-flow components.
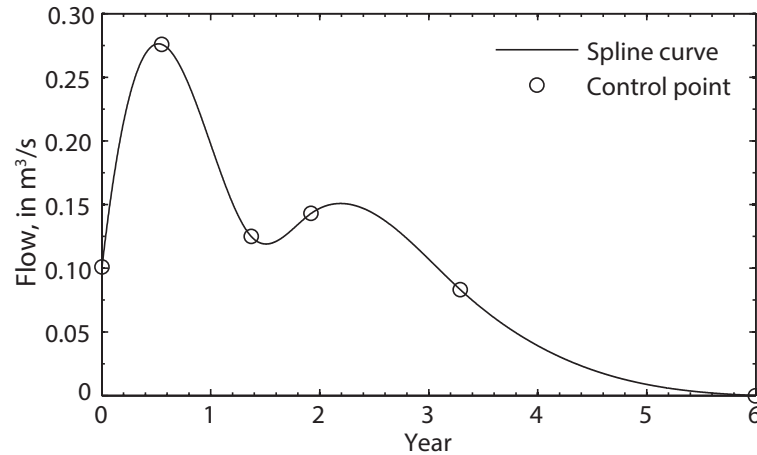
Figure 4. Impulse-response function defined by a spline curve fit through control points.
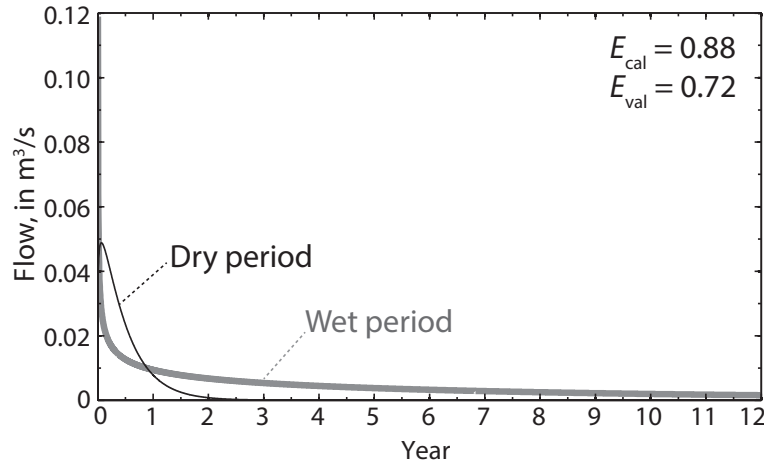
Figure 5. Example F5: impulse-response function (IRF) for Barton Springs using a single-gamma IRF for both periods; i.e., wet and dry. Parameter values are shown in Table 3.

Figure 6. Example F5: observed and simulated springflow for Barton Springs.
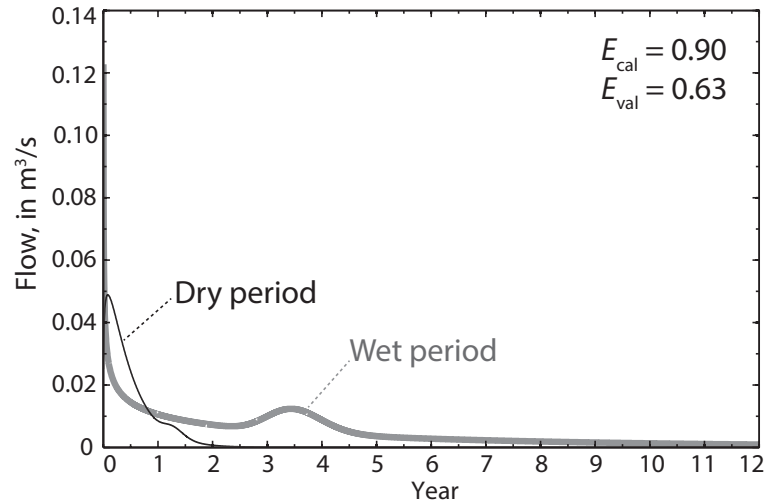
Figure 7. Example F7: impulse-response function (IRF) for Barton Springs using a double-gamma IRF for both periods; i.e., wet and dry. Parameter values are shown in Table 3.

Title Page

Abstract | Introduction

Conclusions | References

Tables | Figures

|◄ | ►|

◄ | ►

Back | Close

Full Screen / Esc

Printer-friendly Version

Interactive Discussion

Full Screen / Esc
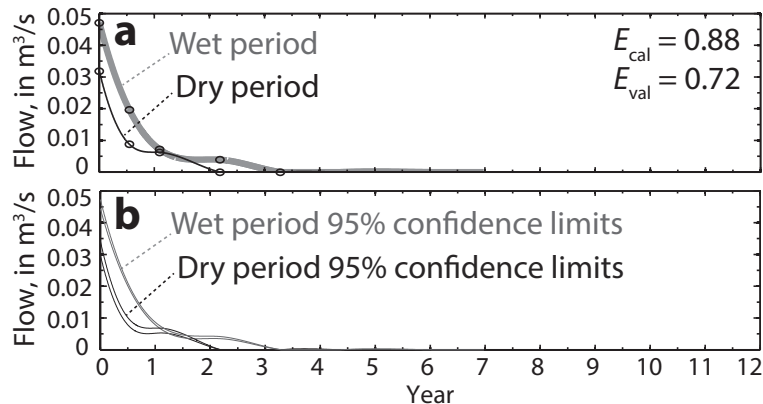
Figure 8. Example F8: nonparametric impulse-response functions (IRFs) for Barton Springs using a total of 7 control points showing **(a)** optimized IRFs and **(b)** upper and lower 95 % confidence limits.

$E_{cal} = 0.92$
$E_{val} = 0.61$

Wet period

Dry period
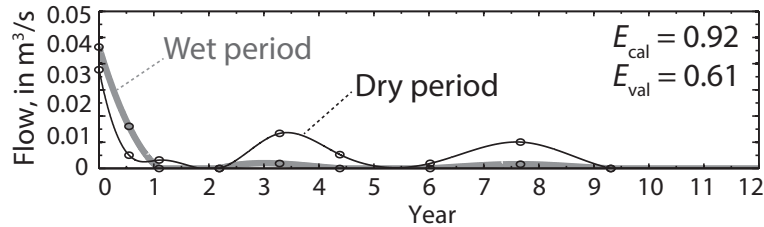
Figure 9. Example F9: nonparametric impulse-response functions for Barton Springs using a total of 16 control points.

Full Screen / Esc

Printer-friendly Version

Interactive Discussion
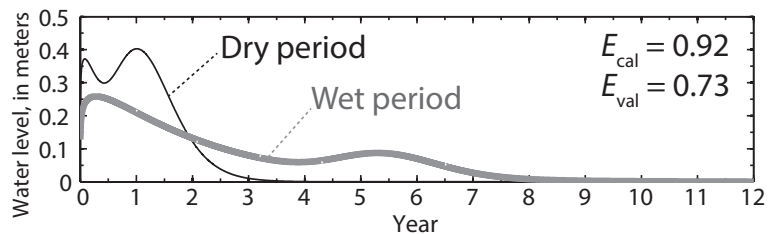
Figure 10. Example F10: impulse-response functions (IRFs) for well LA88C using double-gamma IRFs for both periods; i.e., wet and dry. Parameter values are shown in Table 3.
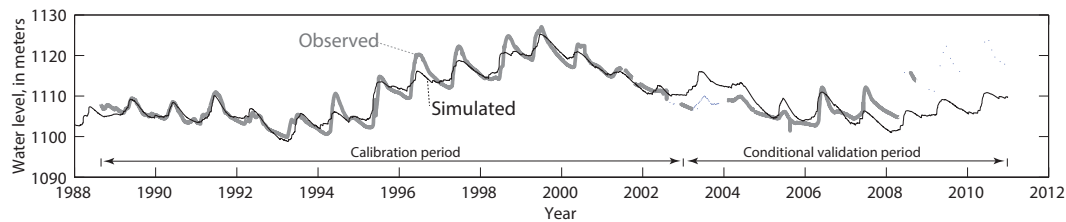
Figure 11. Example F10: observed and simulated water level for well LA88C.
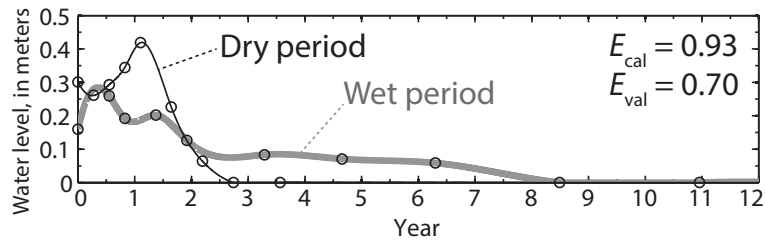
Figure 12. Example F12: nonparametric impulse-response functions for well LA88C using a total of 18 control points.
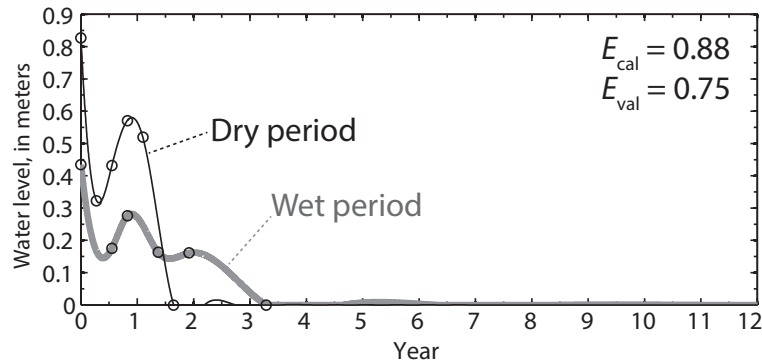
Figure 13. Example F13: nonparametric impulse-response functions for well LA88C using a total of 10 control points.